

## **Polycyclic Aromatic Hydrocarbons in Coarse Fly Ash Particles Emitted from Fluidized-bed Combustion of Thai Rice Husk**

**Kasama Janvijitsakul\* , Vladimir I. Kuprianov**

School of Manufacturing Systems and Mechanical Engineering, Sirindhorn International Institute of Technology, Thammasat University, Pathum Thani, Thailand

\*Author to whom correspondence should be addressed, email: [kasama@siit.tu.ac.th](mailto:kasama@siit.tu.ac.th)

---

**Abstract:** This work aimed to study the size distribution of polycyclic aromatic hydrocarbons (PAHs) in the fly ash emitted from a fluidized-bed combustor firing Thai rice husk. The particle size distribution and chemical composition of the fly ash are discussed. More than 80% of ash particles were found to have the volume mean diameter of 11 to 260  $\mu\text{m}$ . SEM images of some fine and coarse particles are presented. The fine particles were found to show a tubular-shaped and polish-structured surface, while the coarse particles basically exhibited a hydroscopic-pores surface texture. Concentrations of eleven PAHs (naphthalene, phenanthrene, anthracene, fluoranthene, pyrene, benzo[b]fluoranthene, benzo[k]fluoranthene, benzo[a]pyrene, dibenzo[a,h]anthracene, indeno[1,2,3-cd]pyrene, benzo[g,h,i]perylene) were quantified for three groups of particle size, 0.5–125  $\mu\text{m}$ , 125–150  $\mu\text{m}$  and 150–250  $\mu\text{m}$ . The total PAH concentration was found to be quite substantial (271.6  $\mu\text{g}/\text{kg}$ ) in the 150–250  $\mu\text{m}$  particles, while it was dramatically reduced with smaller particle size. The highest concentrations were observed for the most toxic compounds, benzo[a]pyrene, indeno[1,2,3-cd]pyrene and benzo[g,h,i]perylene

**Keywords:** Particle Size, SEM Images, Surface Texture, Size Distribution, Total PAH Concentration

---

### **Introduction**

For many years, biomass has been an important renewable source for heat and power generation. Stoker firing and fluidized bed combustion systems have been widely used for energy conversion from biomass. By recent time, most of research studies related to emissions from biomass combustion have been devoted to inorganic pollutants,  $\text{NO}_x$ ,  $\text{N}_2\text{O}$ ,  $\text{SO}_2$ ,  $\text{CO}$  and  $\text{CO}_2$ . However, some works have been addressed the emissions of volatile organic compounds and polycyclic aromatic hydrocarbons (PAHs) from closed-type combustion systems (boilers and combustors) and open burnings.

Polycyclic aromatic hydrocarbons (PAHs) are known to be a family of volatile, semi-volatile and non-volatile organic species made up of carbon and hydrogen atoms. Basically, they are formed on the initial stage of the combustion, following devolatilization of fuel particles. Upon heating, methane, acetylene and other organic volatile compounds are partially cracked to smaller unstable free radicals. During recombination, the radicals form various PAHs with two or more aromatic rings [1–3]. Some PAHs with greater number of aromatic rings (or with higher molecular weight), such as benzo[*a*]anthracene, chrysene, benzo[*b*]fluoranthene, benzo[*a*]pyrene, indeno[1,2,3-*cd*]pyrene, dibenz[*a,h*]anthracene, are known to be strong carcinogens and mutagens [1,4–6].

Basically, PAHs emitted from combustion systems are present in two phases of combustion products, particulate matter and gaseous phase. Low molecular weight (2- and 3-ring) PAHs, such as naphthalene, acenaphthylene, phenanthrene and fluoranthene, are generally associated with gaseous combustion products, whereas higher molecular weight (4-, 5- and 6-ring) PAHs are primarily emitted via fly ash and soot particles, commonly termed particulate matter [7–8]. As the most toxic PAHs belong to the group of nonvolatile (5-ring and larger) PAHs, the distribution of them over the ash particle size is a key issue (objective) in studies dealing with the PAH emissions from biomass combustion.

During the recent decade, a significant number of research works have been carried out on PAHs emissions from various combustion systems firing some biomass fuels and (co-)firing pulverized coal with wood residues [7–13]. The major goals pursued in most of these works have been related to the effects of operating conditions and/or ash particle size and on the yield of different PAHs as well as on the total PAH concentration. However, as follows from the literature review, there is an apparent lack of data on PAH emissions from the fluidized bed combustion of rice husk, one of the most viable renewable energy sources in many Asian countries.

This work was aimed at quantifying the concentrations of sixteen PAHs emitted from fluidized bed combustion of Thai rice husk via fly ash. The effect of the ash particle size on the concentration of different PAHs, as well as on the total PAH concentration, was the main focus of this experimental study.

## Materials and Methods

### *Ash characterization*

To achieve the main objectives of this work, the fly ash was generated during the combustion of Thai rice husk in a fluidized-bed combustor with a cone-shaped bed [14] using corundum (95.4% Al<sub>2</sub>O<sub>3</sub>) as the inert bed material. In this run, the rice husk was supplied into the combustor at the fuel feed rate of 82.4 kg/h and excess air of about 60% was secured. Due to these operating conditions, the temperature of 750–780°C was observed in the combustor.

Table 1 shows the proximate and ultimate analysis of the rice husk. the fuel-ash content seen to be at a substantial level, which results in elevated emissions of particulates from the combustion of this biomass fuel.

For general size characterization of ash particles in a sample, the fly ash was analyzed using the “Mastersizer S” particle size analyzer. In this analysis, the measuring system was set up for the standard range (0.05–900 μm) of the volume mean diameter, which was determined within ± 2% errors. As the result, the particle size was represented in terms of volume mean diameter, while the concentration of ash particles for each particle size (or size fraction) was obtained as the percentage of particles with given size in the total number of ash particles in the sample.

**Table 1** Ultimate and proximate analyses of Thai rice husk

Fuel analysis (wt.%, as-recieved)	Value
Ultimate analysis:	
Carbon	37.8
Hydrogen	5.20
Oxygen	39.0
Nitrogen	0.31
Sulphur	0.05
Proximate analysis:	
Moisture content	11.00
Ash content	17.64

Fig. 1 shows the particle size distribution in a sample of the tested fly ash. As seen in Fig. 1, the total percentage of coarse particles in the sample is predominant. More than 60% of the particles were found to have 48–260  $\mu\text{m}$  volume mean diameters, and over 80% were characterized with the mean diameter of 11 to 260  $\mu\text{m}$ . As followed from this analysis, the mean particle size (termed as the volume mean diameter, averaged over the entire size range, 0.5–477  $\mu\text{m}$ ) was about 130  $\mu\text{m}$ .

Prior to characterization of chemical composition of fly ash and PAH analysis, including the size distribution of fly ash constituents and PAHs, the ash particles were fractioned into three groups with different ranges of the volume mean diameter of particles ( $d_p$ ): (1)  $0.5 < d_p \leq 125 \mu\text{m}$ , (2)  $125 < d_p \leq 150 \mu\text{m}$  and (3)  $150 < d_p \leq 250 \mu\text{m}$ . After segregation, an ash sample of each group was prepared in accordance with requirements of procedures in studies on major elemental compositions and surface morphology of the fly ash as well as for determining PAH concentrations. Table 2 shows the chemical composition of the fly ashes collected from the fluidized-bed combustor firing Thai rice husk for different ranges of the particle size. The (weight) percentages of different ash constituents (oxides) in

Table 2,  $\text{SiO}_2$ ,  $\text{Al}_2\text{O}_3$ ,  $\text{TiO}_2$ ,  $\text{Fe}_2\text{O}_3$ ,  $\text{CaO}$ ,  $\text{MgO}$ ,  $\text{Na}_2\text{O}$ ,  $\text{K}_2\text{O}$ ,  $\text{P}_2\text{O}_5$ ,  $\text{MnO}_5$ ,  $\text{SO}_3$ , were normalized to 100%. The ash analyses were obtained based on the ASTM method (D5142), using the x-ray fluorescence technique. As may be seen in Table 2,  $\text{SiO}_2$  and  $\text{Al}_2\text{O}_3$  are the major components of the fly ash accounting for 91–94% by weight. It appeared that, in general, the individual oxides had rather uncertain correlations with the particle size; however, some oxides (e.g.  $\text{Al}_2\text{O}_3$ ,  $\text{F}_2\text{O}_3$ ,  $\text{K}_2\text{O}$ ) showed apparent trends with increasing the particle size.

### **SEM analysis of ash particles**

The scanning electron microscope (SEM) was used to observe the surface morphology of fly ash by JEOL scanning microscopes (JSM-5800 LV). Prior to this study, the sample particles were coated with gold. The SEM observations at low ( $\times 100$ ) and medium ( $\times 250$  and  $300$ ) magnifications were carried out with the aim to study a general structure of the fly ash for the three size fractions, whereas the high magnification ( $\times 1000$ ) was applied to display the surface texture of ash particles.

### **Sample preparation and PAHs analysis**

Two-gram sample of fly ash of each size fraction was extracted by mixing with 40-ml dichloromethane (DCM) and placing in the ultrasonic bath for 10 minutes. The extracted DCM was then exchanged with 100- $\mu\text{l}$  dimethylsulfoxide (DMSO) and concentrated by purging with ultra-pure nitrogen for cleanup. During the cleanup procedure, the sample was pretreated by using the silica cartridge (Sep-Pak cartridge for solid phase extraction) and then eluted with 2.0 and 3.0 ml of hexane-

dichloromethane (2:1 by volume). After the cleanup procedure, the collected eluant was exchanged with 30- $\mu$ l DMSO and, afterwards, concentrated by purging with ultrapure nitrogen again.

The PAH concentrations were determined using High Performance Liquid Chromatography (HPLC) with the programmable fluorescence detector and diode array detector. The HPLC system was calibrated for sixteen PAHs: naphthalene (Np), acenaphthylene

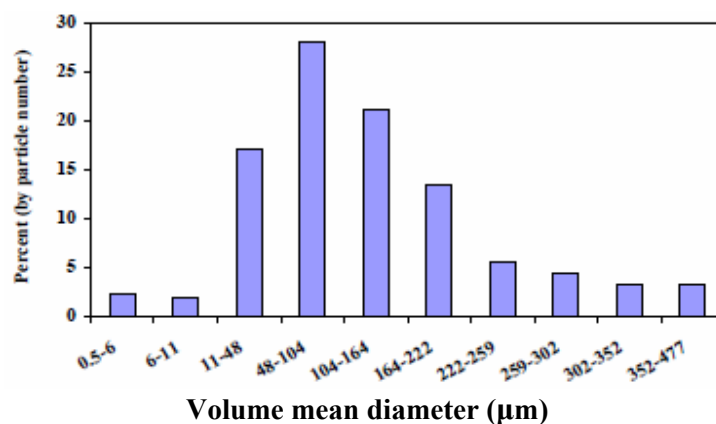


**Fig 1** Particle size distribution of fly ash generated from the conical FBC firing rice husk at fuel feed rate 82.4 kg/h and excess air 60%

**Table 2** Ash analyses for samples with different particle sizes collected from the fluidized-bed combustor firing Thai rice husk

Particle size ( $\mu$ m)	Normalized ash analysis (wt. %)										
	SiO <sub>2</sub>	Al <sub>2</sub> O <sub>3</sub>	TiO <sub>2</sub>	Fe <sub>2</sub> O <sub>3</sub>	CaO	MgO	Na <sub>2</sub> O	K <sub>2</sub> O	P <sub>2</sub> O <sub>5</sub>	MnO <sub>2</sub>	SO <sub>2</sub>
0.5-125	90.00	1.35	0.09	5.31	0.55	0.25	0.14	1.79	0.39	0.11	0.02
125-150	91.17	2.28	0.12	3.25	0.41	0.19	0.21	2.04	0.23	0.08	0.02
150-250	91.07	2.80	0.10	2.06	0.45	0.18	0.20	2.79	0.24	0.08	0.02

(Acn), acenaphthene (Ace), fluorene (F), phenanthrene (Ph), anthracene (An), fluoranthene (Fl), pyrene (Py), benz[a]anthracene (B[a]An), chrysene (Chry), benzo[b]fluoranthene (B[b]Fl), benzo[k]fluoranthene (B[k]Fl), benzo[a]pyrene (B[a]Py), dibenz[a,h]anthracene (D[a,h]An), indeno[1,2,3-cd]pyrene (IPy), benzo[g,h,i]perylene (B[ghi]Pe) in acetonitrile). Though all the PAHs were identifiable, the concentrations of four PAHs, Acn, Ace, F, B[a]An and Chry, were lower than the detection limit and, therefore, were omitted in the discussion below.

## Results and Discussion

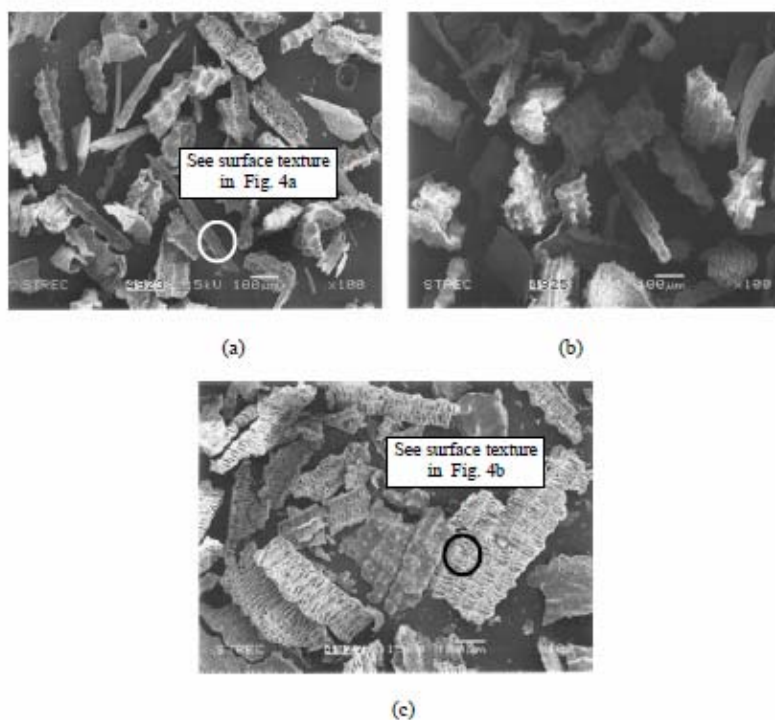
### Surface morphology of fly ash

Fig. 2 shows the SEM images of the fly ash at  $\times 100$  magnification for the three difference particle size fractions. As seen in Fig. 2a, due to the wide range of the particle size, both tubular- or needle-shape particles, as well as small amount of porous-sight particles were found in the fly ash with  $0.5 < d_p \leq 125 \mu$ m. In the ash sample with  $125 < d_p \leq 150 \mu$ m, the porous-sight particles with some amount of needle-shape particles were basically represented (see Fig. 2b). In the fraction with coarsest particles ( $150 < d_p \leq 250 \mu$ m), all the particles were exhibited by porous-sight particles (see in Fig. 2c).

In these observations, the SEM images with low ( $\times 100$ ) magnification were obtained with the aim to display the general shape/geometrical characterization of the fly ash of each size groups, while the images with higher ( $\times 250$ ,  $\times 300$  and  $\times 1000$ ) magnifications were used to study the morphology of ash

surfaces. As an illustration, Fig. 3 shows the SEM images of the particles obtained with the  $\times 250$  and  $\times 300$  magnifications.

The surface morphology of needle-shape and hydroscopic-pore particles are shown in Fig.4. The SEM images represented in Figs. 4a and 4b were obtained with the  $\times 1000$  magnification. As seen in Fig.4a, the tubular-shape particles dominating in the smallest size fraction exhibited the polish-structure surface, while the porous-sight particles in Fig. 4b showed the complex structure with more developed (larger) internal surface area.



**Fig. 2** SEM images (with  $\times 100$  magnification) of fly ash particles of Thai rice husk for the different ranges of the particle size,  $0.5 < d_p \leq 125 \mu\text{m}$  (a),  $125 < d_p \leq 150 \mu\text{m}$  (b) and  $150 < d_p \leq 250 \mu\text{m}$  (c). The surface textures of some fragments in these images can be observed in Fig. 4

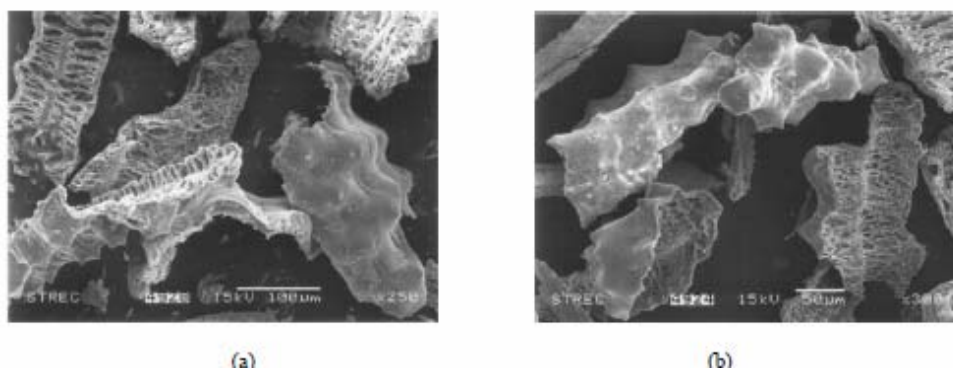


**Fig. 3** SEM images of fly ash particles with  $\times 250$  (a) and  $\times 300$  (b) magnifications.

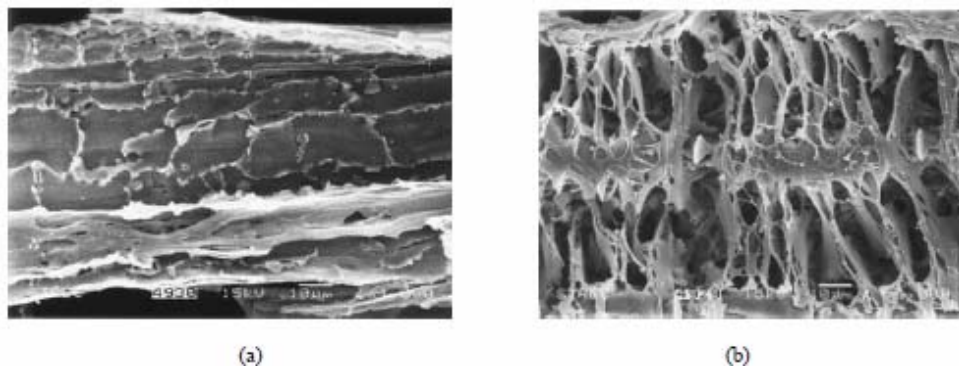


**Fig. 4** SEM images of the surface texture with the tubular-shape (a) and hydroscopic pore(b) structures

**Size distribution of PAHs in fly ash**

Fig. 5 shows the concentrations of naphthalene, phenanthrene, anthracene, fluoranthene, pyrene, benzo[b]fluoranthene, benzo[k]fluoranthene, benzo[a]pyrene, dibenz[a,h]anthracene, indeno[1,2,3-cd]pyrene and benzo[g,h,i]perylene in the fly ash of Thai rice husk (in  $\mu\text{g}$  per kg ash) for different ranges of the particle size.

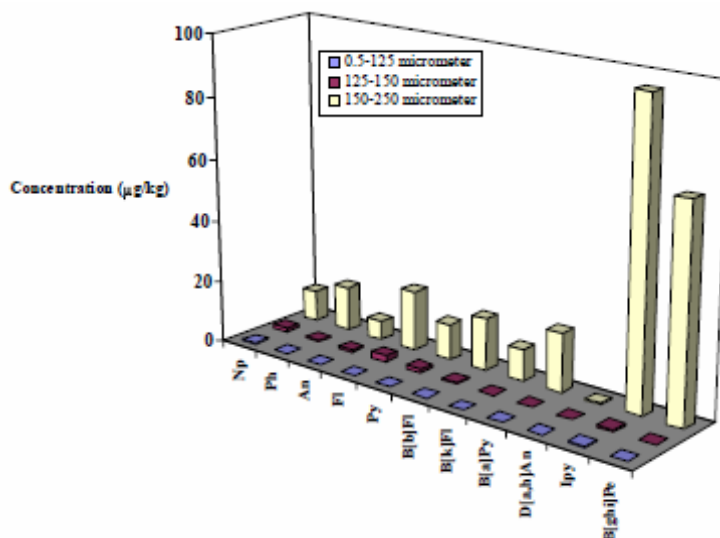


**Fig. 5** Effects of the particle size on the PAH concentration in fly ash generated in a fluidized-bed combustor firing rice husk at the fuel feed rate 82.4 kg/h and excess air 60%

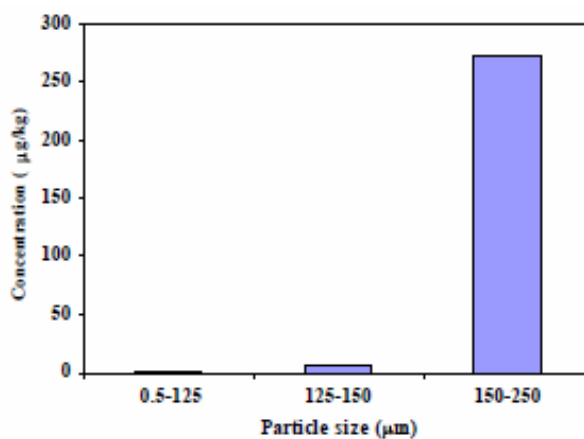


**Fig. 6** Effects of the particle size on the total PAH concentration in fly ash generated in a fluidized-bed combustor firing rice husk at the fuel feed rate 82.4 kg/h and excess air 60 %

As seen in Fig. 5, the highest concentration for each PAH compound was found in the coarsest particles ( $150 < d_p \leq 250 \mu\text{m}$ ). Meanwhile, among these eleven PAHs, the absolute maximum concentration was found for indeno[1,2,3-*cd*]pyrene,  $96 \mu\text{g}/\text{kg}$ , followed by benzo[*g,h,i*]perylene,  $68 \mu\text{g}/\text{kg}$ . Other PAHs showed apparently lower concentration values. Meanwhile, in the ash particles with  $125 < d_p \leq 150 \mu\text{m}$ , the concentration of the particular PAH was significantly lower than that in the coarsest particles. Highest concentrations in fly ash with  $125 < d_p \leq 150 \mu\text{m}$  were exhibited by fluoranthene ( $2.2 \mu\text{g}/\text{kg}$ ), naphthalene ( $1.4 \mu\text{g}/\text{kg}$ ) and pyrene ( $1.2 \mu\text{g}/\text{kg}$ ). The concentrations of other PAHs were negligible. For the size range  $0.5 < d_p \leq 125 \mu\text{m}$ , all the PAH concentrations were found to be at negligible level ( $< 0.6 \mu\text{g}/\text{kg}$ ). In ash particles of this size fraction, indeno[1,2,3-*cd*]pyrene and naphthalene showed the highest concentrations,  $0.6 \mu\text{g}/\text{kg}$  and  $0.4 \mu\text{g}/\text{kg}$ , respectively. Fig. 6 shows the total PAH concentration (combining the values of all the PAHs) for the three size fractions. As seen in Fig. 6, the total concentration in the fraction with coarsest particles,  $271.6 \mu\text{g}/\text{kg}$ , was significantly higher compared to  $7.1 \mu\text{g}/\text{kg}$  for  $125 < d_p \leq 150 \mu\text{m}$ , and  $1.3 \mu\text{g}/\text{kg}$  for  $0.5 < d_p \leq 125 \mu\text{m}$ . This fact could be explained by the highly developed “internal” surface of coarsest particles with the hydroscopic pore structure (see Fig. 4b); accordingly, greater amounts of PAH could be condensed on the internal surface of these particles and transported with them.

Fig. 7 shows the total PAH concentration versus the number of aromatic rings in PAHs (naphthalene is a 2-ring PAH; phenanthrene and anthracene are 3-ring PAHs; fluoranthene and pyrene are 4-ring PAHs; benzo[*b*]fluoranthene, benzo[*k*]fluoranthene, benzo[*a*]pyrene and dibenz[*a,h*]anthracene are 5-ring PAHs; indeno[1,2,3-*cd*]pyrene and benzo[*g,h,i*]perylene are 6-ring PAHs) for the coarsest particles. As seen in Fig. 7, benzo[*b*]fluoranthene, benzo[*k*]fluoranthene, benzo[*a*]pyrene, indeno[1,2,3-*cd*]pyrene and benzo[*g,h,i*]perylene (or 5- and 6-ring PAHs), i.e. species high carcinogenic potential PAHs, were found to be predominant, with the total concentration of these five species  $212.1 \mu\text{g}/\text{kg}$ . However, these high toxic species can be captured together with the fly ash particles in cyclones or baghouses. Since these non-volatile PAHs are basically bonded with ash particles, the concentrations in Figs. 5–7 can be used for quantifying the actual PAH emissions from the combustion system, using the size distributions of PAH concentrations and mass fractions of the fly ash. However, 2- and 3-ring PAHs, such as naphthalene, phenanthrene and anthracene, are expected to emit from the combustion system via flue gas phase. For accurate determination of emission characteristics for these volatile PAHs, the reliable data on their concentration in the flue gas is required.

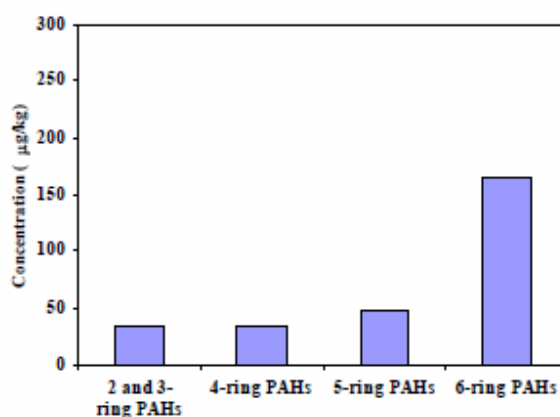


**Fig. 7** Total PAH concentration versus the number of aromatic rings in PAHs emitted via fly ash from the fluidized-bed combustor firing rice husk at the fuel feed rate  $82.4 \text{ kg}/\text{h}$  and excess air 60%

## Conclusions

Concentrations of eleven PAHs (naphthalene, phenanthrene, anthracene, fluoranthene, pyrene, benzo[*b*]fluoranthene, benzo[*k*]fluoranthene, benzo[*a*]pyrene, dibenzo[*a,h*]anthracene, indeno[*1,2,3-cd*]pyrene and benzo[*g,h,i*]perylene) in fly ash of rice husk have been quantified for three groups of the particle size (or volume mean diameter,  $d_p$ ):  $0.5 < d_p \leq 125 \mu\text{m}$ ,  $125 < d_p \leq 150 \mu\text{m}$  and  $150 < d_p \leq 250 \mu\text{m}$ . The fly ash used in this study has been generated in a fluidized-bed combustor firing 82.4 kg/h of Thai rice husk (with the elevated fuel-ash content) at excess air 60%.

Prior to the PAH analysis, the chemical composition, particle size distribution and surface texture of ash particles have been investigated. As follows from ash analysis, total  $\text{SiO}_2$  and  $\text{Al}_2\text{O}_3$  content in the fly ash of the rice husk is predominant, accounting for 91–94% (by weight). More than 80% of the ash particles are characterized by the volume mean diameter of 11 to 260  $\mu\text{m}$ , i.e. can be generally treated as the coarse particles. Basically, the finer (0.5–125  $\mu\text{m}$ ) ash particles exhibit a tubular-shaped and/or polishstructured surface, while the coarsest (150–250  $\mu\text{m}$ ) particles show a hygroscopic-pores surface texture.

As revealed by the PAH analysis, there is a strong effect of the particle size on the PAH concentrations. For the particular PAH compound, the highest concentration is related to coarsest particles ( $150 < d_p \leq 250 \mu\text{m}$ ). In this size fraction, the absolute maximum concentration is exhibited by indeno[*1,2,3-cd*]pyrene, 96  $\mu\text{g}/\text{kg}$ , followed by benzo[*g,h,i*]perylene, 68  $\mu\text{g}/\text{kg}$ . Other PAHs show apparently lower concentration values. For the particles of another two groups (of smaller size), the concentrations are significantly lower or, for some PAHs, negligible. As the result, the total PAH concentration in coarsest ( $150 < d_p \leq 250 \mu\text{m}$ ) particles of the rice husk is significantly higher compared to those for smaller size groups.

The contribution of the 5- and 6-ring PAHs (benzo[*b*]fluoranthene, benzo[*k*]fluoranthene, benzo[*a*]pyrene, indeno[*1,2,3-cd*]pyrene and benzo[*g,h,i*]perylene), i.e. species high carcinogenic potential PAHs, to the total PAH concentration is predominant. However, these high toxic species can be captured together with the fly ash particles in cyclones or baghouses

## Acknowledgments

The authors would like to acknowledge the financial support from the Royal Golden Jubilee Ph.D. Program, the Thailand Research Fund, Contracts No.PHD/0051/2546 and No. BGJ47K0006.

## References

- [1] Agency for Toxic Substances and Disease Registry. (1995) *Toxicological profile for polycyclic aromatic hydrocarbons (PAHs)*, Atlanta, GA: U.S. Department of health and human services, Public health service.
- [2] Leclerc, D., Duo, W.L.V. and Vessey, M. (2006) Effects of combustion and operating conditions on PCDD/PCDF emissions from power boilers burning salt-laden wood waste, *Chemosphere*, **63**, pp. 676–689.
- [3] Hazardous Substances Data Bank. (1994) *National library of medicine*, National toxicology program (via TOXNET), Bethesda, MD.
- [4] Rybickia, B.A., Nockb, N.L., Saverac, A.T., Tangd, D. and Rundle, A. (2006) Polycyclic aromatic hydrocarbon-DNA adduct formation in prostate carcinogenesis, *Cancer Letters*, **239**, pp. 157–167.

- [5] Knafla, A., Phillipps, K.A., Brecher, R.W., Petrovic, S. and Richardson M. (2006) Development of a dermal cancer slope factor for benzo[a]pyrene, *Regulatory Toxicology and Pharmacology*, **45**, pp. 159–168.
- [6] Okona-Mensah, K.B., Battershill, J., Boobis, A. and Fielder, R. (2005) An approach to investigating the importance of high potency polycyclic aromatic hydrocarbons (PAHs) in the induction of lung cancer by air pollution, *Food and Chemical Toxicology*, **43**, pp. 1103–1116.
- [7] Mastral, A.M., Callen, M., Mayoral, C. and Galbfin, J. (1995) Polycyclic aromatic hydrocarbon emissions from fluidized bed combustion of coal. *Fuel*, **74**, (12), pp. 1762–1766.
- [8] Cabanas, A., Saez, F., Gonzalez, A. and Escalada, R. (2000) Quantitative assessment of polycyclic aromatic hydrocarbons from corckwaste combustion emission, *Journal of Agricultural Engineering Research*, **77**, (3), pp. 349–354.
- [9] Gulyurtlu, I., Karunaratne, D.G.G.P. and Cabrita, I. (2003) The study of effect of operating parameters on the PAH formation during the combustion of coconut shell in a fluidised bed, *Fuel*, **82**, pp. 215–223.
- [10] Jenkins, B.M., Jones, A.D., Turn, S.Q. and Williams, R.B. (1996) Particle concentrations gas-particle partitioning and speices intercorrelations for polycyclic aromatic hydrocarbons (PAH) emitted ducring biomass burning, *Atmospheric Environment*, **30**, (22), pp. 3825–3835.
- [11] Ross, A.B., Jones, J.M., Chaiklangmuang, S., Pourkashanian, M., Williams, A., Kubica, K., Andersson, J.T., Kerst, M., Danihelka, P. and Bartel K.D. (2002) Measurement and prediction of the emission of pollutants from the combustion of coal and biomass in a fixed bed furnace, *Fuel*, **81**, pp. 571–582.
- [12] Johansson, L.S., Leckner, B., Gustavsson, L., Cooper, D., Tullina, C. and Potter, A. (2004) Emission characteristics of modern and old-type residential boilers fired with wood logs and wood pellets, *Atmospheric Environment*, **38**, pp. 4183–4195.
- [13] Saez, F., Cabanas, A., Gonzalez, A., Martinez, J.M., Rodriguez, J. J., Dorronsoro, J. L. (2003) Cascade impactor sampling to measure polycyclic aromatic hydrocarbon from biomass combustion process, *Biosystems Engineering*, **86**, (1), pp.103–111.
- [14] Koupryanov, V.I., and Permchart, W. (2003). Emission from a conical FBC fired with a biomass fuels, *Applied Energy*, **74** (3–4), pp. 383–392.
- [15] Arditsoglou, A., Petaloti, C., Terzi, E., Sofoniou, M. and Samara, C. (2004) Size distribution of trace elements and polycyclic aromatic hydrocarbons in fly ashes generated in Greek lignite-fired power plants, *Science of the Total Environment*, **323**, pp. 153–167.
- [16] Griest, W.H., Yeatts, L.B. and Caton, J.E. (1980) Recovery of polycyclic aromatic hydrocarbons sorbed on fly ash for quantitative determination, *Anal. Chem*, **52**, pp. 199–201.